Conf-921201--12

58918-00-105 MANUSCRIPT September 1992

# MAGNETIC COUPLING OF Fe/Mo/Fe AND Co/Cu/Co SANDWICHES ACROSS WEDGED SPACER LAYERS*

ANL/CP--76470

DE93 004203

Z.Q. Qiu, J. Pearson, and S.D. Bader

*Materials Science Division*
*Argonne National Laboratory, Argonne, IL 60439*



**37th Magnetism and Magnetic Materials Conference, Houston, Texas, December 1-4, 1992, Proceedings to be published in Journal of Applied Physics**

jmc

## DISCLAIMER





*Research supported in by the U.S. Department of Energy under contract #W-31-109-ENG-38.

# Magnetic Coupling of Fe/Mo/Fe and Co/Cu/Co Sandwiches Across Wedged Spacer Layers (INVITED)

*Z. Q. Qiu, J. Pearson, and S. D. Bader*

*Material Science Division, Argonne National Laboratory, Argonne, IL 60439.*

Fe/Mo/Fe and Co/Cu/Co sandwiches were grown by molecular beam epitaxy onto Mo(100) and Cu(100) single crystals, respectively, and characterized by high- and low-energy electron diffraction and *in-situ* surface magneto-optic Kerr-effect measurements. The spacer layer in both case was fabricated to have a wedged shape in order to create a continuous change of the spacer-layer thickness. Oscillatory behavior between ferromagnetic and antiferromagnetic coupling was found; and is shown to originate at the interface between the magnetic layer and the spacer layer. For Fe/Mo/Fe, short-period oscillations are observed with a periodicity of ~3ML of Mo. Hysteresis loops for antiferromagnetically coupled cases are calculated from a simple model, and the results reproduce the general characteristics observed experimentally.

PACS numbers: 75.50.Rr, 75.60.Ej, 75.70.Ak, 75.70.Cn

## I. Introduction

Antiferromagnetic (AF) coupling between two magnetic layers across intervening nonmagnetic layer as found in Fe/Cr sandwiches has stimulated a greal deal of activity within the materials physics community.[1] The discovery of giant magnetoresistance in Fe/Cr sandwiches and superlattices[2], in particular, also has high potential for applications in magnetic recording. These developments have generated an interest in the underlying mechanisms associated with the magnetic coupling. The studies indicate that the magnetic coupling not only changes its strength but also exhibits oscillatory behavior between AF- and ferromagnetic-coupling as a function of the Cr thickness. This suggests that the coupling is due to a Rudermann-Kittel-Kasuya-Yosida (RKKY)-type interaction. Many other systems were found to behave similarly to Fe/Cr, such as Fe/Cu,[3] Fe/Mo,[4] Co/Ru,[5] Co/Cr,[5] and Co/Cu.[6], *etc.* All of these systems exhibit oscillatory behavior between AF and ferromagnetic coupling, with the oscillation periodicity of ~10Å thickness of the nonferromagnetic component, except for Cr, whose period is ~18Å. These periods are much longer than the RKKY periodicity of $\pi/k_F$, where $k_F$ is the magnitude of the Fermi vector of the nonmagnetic component. Theoretical analysis indicates that because of the discrete atomic structure within the layers, the oscillatory periodicity in the sandwich and superlattice structures should be $\pi/|\mathbf{k}_{BZ}-\mathbf{k}_F|$ instead of $\pi/k_F$, where $k_{BZ}$ is the magnitude of the vector to the Brillouin zone boundary in the normal direction of the film.[7,8] The new results not only successfully reproduced the observed long-period oscillations, but also predict the existence of short-period (~1-3ML) oscillations. Experimental observation of the short periodicity requires extreme surface flatness and precise control of interlayer thickness, since a surface roughness or an error in thickness comparable to the short periodicity will eliminate such oscillations. Molecular beam epitaxy (MBE) provides the ability to grow single-crystalline films with only atomic-scale surface roughness; therefore MBE has been employed frequently in the search of short-period oscillations. Two systems, Fe/Cr[9,10] and Fe/Mn[11], were the first found to exhibit short-

period (~2ML) oscillations. The samples of both of those systems were fabricated by evaporation onto flat Fe whiskers, and the non-ferromagnetic spacer layer was grown using a moving mask to form a wedge. The advantage of making wedge samples is to provide a continuous change of the spacer-layer thickness so that a probe beam can measure the magnetic coupling for different thicknesses of the spacer layer in a systematic way as it scans across the sample. Short-period oscillations were found later in wedged samples of the Fe/Au,[12] Fe/Mo,[13] Fe/Ag[14] and Co/Cu[15] systems.

The first part of this paper, will provide a review of our study of the Fe/Mo system to explore short-period oscillations. Another issue addressed in this paper concerns the coupling mechanism between the magnetic and the nonmagnetic layers. Most theoretical models assume that the coupling occurs only at the interface between the two layers, and, therefore, constrain the thickness of the magnetic layer, for convenience, to be only 1 monolayer (ML). The consequence of this assumption is that the interlayer coupling strength and the oscillation periodicity should be independent of the magnetic layer thickness. It is important to test this assumption experimentally. That is the second goal of the present work. Our investigation is recounted of the epitaxial Co/Cu/Co sandwich system[16] grown onto Cu(100) by MBE with a wedge-shaped Cu spacer layer. This system is used to explore the relationship between the AF coupling and the thickness of the magnetic layers. Lastly, a theoretical calculation is presented for the hysteresis loops of AF-coupled sandwiches. The results reproduce the general characteristics observed in the experiments discussed above.

## II. Experiment

*1. Growth and characterization of the sandwiches*

The Fe/Mo/Fe and Co/Cu/Co sandwiches were grown by MBE onto a Mo(100) and Cu(100) single crystal substrates, respectively, at room temperature in an ultrahigh vacuum (UHV) chamber of base pressure $2\times10^{-10}$ Torr. The chamber is equipped with reflection

high-energy (RHEED) and low-energy electron diffraction (LEED), Auger spectroscopy, an Ar-ion sputtering gun for substrate cleaning, and a UHV-compatible superconducting magnet. The substrates are single crystal disks of ~2mm thickness and ~10mm diameter. The Mo and Cu substrates were mechanically polished to a ~1-μm and 0.1-μm diamond-paste finish, respectively and ultrasonically cleaned in methanol before its introduction into the UHV chamber. Then cycles of 1-3keV $Ar^+$ sputtering and annealing at ~700°C for ~30 minutes were used to improve the surface quality. Auger spectroscopy was used to confirm the cleanliness of the surface. RHEED and LEED indicated that a well defined Mo(100) and Cu(100) surfaces were formed (Fig. 1 and 2) after the above treatments. The Fe, Mo, Co, and Cu layers were grown at room temperature by evaporating Fe, Co wires and Cu rod from alumina crucibles surrounded by W heating wire,[17] and by evaporating a 2mm-diameter Mo wire held at 4 kV from an electron gun whose design is based on that of Jonker.[18]. The pressure during growth remained $<3\times10^{-10}$ Torr.

For the Fe/Mo/Fe sandwiches, a 14-ML Fe film was first grown onto the Mo(100) substrate, followed by the growth of a Mo wedge. The wedge was created by placing a Ta mask above and in front of the specimen to block part of the evaporated Mo beam, and by slowly translating the specimen along the [010] crystal direction behind the mask. The process of making the Mo wedge is illustrated schematically in Fig. 3. For a specimen motion speed of $v$ and a Mo evaporation rate of $r$, the Mo wedge has a thickness gradient of $r/v$. The slope of the Mo wedge can be precisely determined by controlling $v$. Typical values of the slope of a wedge are ~1-2Å/mm. After the growth of the Mo wedge, another 14-ML Fe film was deposited to complete the sandwich structure. Subsequent annealing of the sample at 150°C for ~30 min. improved the surface smoothness. Four samples were fabricated in this manner to cover the Mo thickness range of 1-18ML. The RHEED and LEED patterns of Fig. 1 show that the Fe/Mo/Fe sandwich forms as a (100)-oriented single crystal.

For the Co/Cu/Co sandwiches, three series of samples were made with Co layer thicknesses of 8, 14 and 20 ML. The intervening Cu layer again was made in to a wedged shape with a slope of ~2-4Å/mm. The RHEED and LEED patterns after making the sandwiches are shown in Fig. 2. The growth mode of Co on Cu and Cu on Co was studied by monitoring the RHEED intensity during the growth and the results are shown in Fig. 4. The oscillations in the RHEED intensity demonstrate that both Co on Cu and Cu on Co follow predominantly a layer-by-layer epitaxial growth mode. We also found that the RHEED line spacing for Co on Cu(100) is the same within experimental uncertainty as that of Cu(100), which indicates that the *fcc* Co structure is formed on Cu(100) with the in-plane lattice spacing of Cu (3.61Å). Although we did not obtain the interlayer spacing, Schneider *et al.*[19] performed a LEED intensity analysis for the same system and reported a 1.74-Å spacing, which is ~3% smaller than the corresponding in-plane value. Thus, the resultant *fcc* structure of Co on Cu(100) is tetragonally compressed along the surface normal.

*2. Basic principles of the SMOKE technique*

The magnetic coupling at room temperature between the two magnetic layers across the spacer layer was studied *in situ* by means of the surface magneto-optic Kerr-effect (SMOKE) technique. The basic principles of the SMOKE technique is described herein briefly and was illustrated in an early papers.[20] An incident beam from an intensity-stabilized He-Ne laser was polarized in the plane of incidence (*p*-polarization). After reflection from the specimen, an analyzing polarizer was set at $\delta \sim 1^{o}$ from extinction to give a bias signal (Kerr intensity) and to enhance the signal-to-noise ratio. A quarter-wave plate was used to remove the birefringence of the UHV window, and optical lenses were used to focus both the incident beam onto the sample and the reflected beam onto a photodiode detector. The external magnetic field H was applied in the film plane and in the plane of

incidence (longitudinal Kerr effect). The intensity detected by the photodiode was recorded *vs* H to generate magnetic hysteresis loops.

*3. Short-period oscillation of the magnetic coupling in Fe/Mo/Fe sandwiches.*

The oscillatory behavior was investigated by scanning the laser (beam size <0.2mm) along the length of the wedge and recorded the hysteresis loops at different positions. Since the wedge gradient is ~1-2Å/mm, the thickness variation within the laser spot is <0.4Å. Thus, the Mo thickness can be quite uniform within the laser spot. Five oscillations of the magnetic coupling were observed in the 1-18ML range of Mo thickness. Typical hysteresis loops of the sandwiches are shown in Fig. 5. The nominal Mo thicknesses are denoted at the right side of each loop. It should be mentioned that the magnetization is in the plane of the film and no signal perpendicular to the film plane (polar Kerr effect) was observed in the same magnetic-field range. The hysteresis loops of the ferromagnetically-coupled samples have a low saturation field and a high remanent magnetization. This is expected since the two coupled Fe films are equivalent to a single ferromagnetic Fe film. In contrast, the hysteresis loops of the AF-coupled samples show two loops shifted from the zero field by $H_S$. Examination of Fig. 5 shows that the width of the two loops become somewhat smaller as the switching field $H_S$ becomes larger, and that the plateau region between the offset loops has a finite slope. Detailed discussion of the hysteresis loops of AF-coupled samples will be provided in Sec. III.

The switching field $H_S$ provides a rough measure of the AF-coupling strength, and is plotted in Fig. 6. From Figs. 5 and 6, it can be seen that the oscillation is not only in the *strength* but also in the *sign* of the coupling. (However, we are not able to distinguish between ferromagnetic- and non-coupling cases from the hysteresis loops.[21]) These results differ from those reported in the SMOKE studies for Fe/Cr[10] and Fe/Mn[11] wedged samples, in that the latter exhibited AF coupling with oscillations only in the coupling strength.

Figure 6 shows that the oscillation periodicity is ~3ML of Mo, which suggests that the magnetic coupling is due to an RKKY-type interaction, rather than to a direct exchange interaction. The later would give 2-ML periodicity and would require the extreme assumption that the Mo possess moments and be an antiferromagnet like Cr or Mn. The 3ML (4.7Å) periodicity is much shorter than the periodicity of ~11Å observed in sputtered Fe/Mo superlattices that are (110) textured.[4] This indicates that there exist both short- and long-period oscillations in this system. Another interesting feature is that the first AF peak is observed at ~5ML of Mo. Based on the ~3-ML oscillation periodicity, there should have been another AF-coupling peak at ~2ML of Mo. Its absence could be due to the interfacial roughness between Fe and Mo, since even a 1-ML roughness could produce pinholes in a 2-ML thick Mo layer. Pinholes in the Mo layer would allow the two Fe films to join together into a single ferromagnetic film.

*4. The AF coupling in Co/Cu/Co sandwiches.*

The same method was used to investigate the coupling in Co/Cu/Co sandwiches as was used for the Fe/Mo study. Typical hysteresis loops of ferromagnetically- and AF-coupled Co(20ML)/Cu/Co(20ML) are shown in Fig. 7. Similar to the Fe/Mo system, the hysteresis loops for AF-coupling samples have a plateau in low fields and a rather abrupt switching to the saturation state at high field, resulting in two hysteresis loops shifted from zero field by $\pm H_S$. $H_S$ is used again as an approximate measure of the AF-coupling strength. For ferromagnetic coupling $H_S=0$. In Fig. 8, $H_S$ is displayed as a function of Cu thickness for all three series of samples. Three oscillations in the exchange coupling appear in Fig. 8 with a periodicity of ~5.5ML (9.9Å) of Cu, independent of Co thickness. The 5.5-ML periodicity agrees with one period predicted[8] by the Bruno and Chappert calculation. However, the shorter period (~2.6ML) predicted by that theory was not observed in our experiment, but was observed recently by Johnson *et al.*[15] Different growth conditions were tried in a search for short-period oscillations (*e.g.* changing the

substrate temperature and/or homoepitaxially smoothing the substrate) but all films showed the same ~5.5-ML periodicity. The absence of short-period oscillations may be attributed to interfacial roughness. It is interesting to note that the interface roughness we previously observed for the Fe/Mo system appears to be greater than that of the present system, as indicated by RHEED and LEED studies, but the Fe/Mo/Fe sandwiches exhibited short-period oscillations. Therefore, the present results suggest that the observation of short-period oscillations in the Co/Cu/Co system is more demanding of interfacial perfection than was the case for Fe/Mo/Fe.

To estimate the AF-coupling strength, we used the conventional assumption that the coupling only occurs at the interfaces. This implies that the coupling strength per unit area of interface, $J_{AF}$, is independent of the thickness $d_{Co}$ of the magnetic layer. In this way, the coupling strength easily can be derived from the value of $H_S$. The idea is that at the switching field the magnetic energy of the anti-parallel-alignment configuration is the same as that for parallel alignment of the two Co films. Then we define:

$$J_{AF} \approx M_S H_S d_{Co} ,$$

where $M_S = 1.47 \times 10^3$ emu/cm$^3$ is the saturation magnetization. We see from this equation that if $J_{AF}$ is independent of Co thickness, $H_S$ should be inversely proportional to $d_{Co}$. This trend is illustrated in Fig. 9 where we replotted the data from Fig. 8 as $J_{AF}$ *vs* Cu spacer-layer thickness. Indeed, the three curves from Fig. 8 fall onto a single curve in Fig. 9. This result demonstrates that the coupling occurs at the Co/Cu interfaces and, thus, is independent of $d_{Co}$. In addition, the $1/d_{Cu}^2$ relation in the AF-coupling strength as predicted by RKKY-interaction calculations,[22] can be seen in Fig. 9 (dashed lines).

## III. Calculation of hysteresis loops for AF-coupled sandwiches

From Sec. II, we see that the hysteresis loops for the AF-coupled sandwiches studied herein have the following features:

(1) Each loop includes two side lobes shifted from zero field.

(2) The side lobes become less prominent as the switching field becomes larger.

(3) The plateau region has a small but finite slope.

In this section a calculation is presented of the hysteresis for AF-coupled sandwiches. The calculation reproduces the main features observed experimentally. In the model used we only consider the AF coupling, the crystal anisotropy and the Zeeman contributions to the energetics. In real systems, however, magnetic domain wall movement and its associated energy also play an important role in determining the shape of the hysteresis loop. However, domain wall movement is ignored herein for simplicity.

Consider a [100]-oriented sandwich with two ferromagnetic layers coupled antiferromagnetically, and an external field applied in the film plane and along the easy axis of magnetization. With the magnetization in the film plane, the magnetic energy of the sandwich per unit area is:

$$E=Kd(\sin^2\phi_1\cos^2\phi_1+\sin^2\phi_2\cos^2\phi_2)-M_SdH(\cos\phi_1+\cos\phi_2)+J\cos(\phi_2-\phi_1), \qquad (1)$$

where K, $M_S$, d, and J are the anisotropy constant, saturation magnetization per unit volume within each magnetic layer, the thickness of each magnetic layer, and the AF-coupling strength between the two ferromagnetic layers, respectively.[23] $\phi_1$ and $\phi_2$ are the angles between the magnetization and H of each of the two ferromagnetic layers. The goal is to minimize the energy in Eq. (1). Since H is applied in the easy magnetization direction, it is straightforward to show that the stable solution satisfies $\phi_1=-\phi_2$ (the magnetization of the two ferromagnetic layers is symmetric in orientation relative to the external field direction). Then Eq. (1) can be restated as:

$$E=2Kd(\sin^2\phi\cos^2\phi-h\cos\phi+\frac{j}{2}\cos2\phi)=2Kd[-u_z^4+(j+1)u_z^2-hu_z-j/2] \quad (2)$$

where $\phi=\phi_1=-\phi_2$, $h=HM_S/K$, $j=J/Kd$, and $u_z=\cos\phi=M_z/M_S$. These are convenient quantities to work with because h and j represent reduced field and exchange parameters (scaled by the anisotropy), and $u_z$ is the projection of the magnetization in the field direction, *i.e.*, the measured magnetization. The requirement that $\partial E/\partial u_z=0$ gives the condition to minimize the energy as:

$$-4u_z^3+2(j+1)u_z-h=0 \quad (3)$$

In general, Eq. (3) has three roots which correspond to two local maxima and one local minimum in the E-$u_z$ plane (Fig. 10). The root which gives the minimum is the correct magnetization. As h increases, the roots also change their values. At $h_2=8[(j+1)/6]^{3/2}$, the second and the third roots become degenerate [corresponding to $\partial^2E/\partial u_z^2=0$, and $u_z=[(j+1)/6]^{1/2}$], and the magnetization jumps from $u_z=[(j+1)/6]^{1/2}$ to $u_z=1$ (Fig. 10). As h decreases from $h>h_2$, the magnetization remains saturated until $u_z=1$ becomes the local maximum; at that point [corresponding $h_1=2(j-1)$], the magnetization jumps from $u_z=1$ to $u_z=\{(j/2-1/4)^{1/2}-1/2\}$. This process generates the hysteresis loops (Fig. 7) in the $u_z$-h plane. Two critical points can be identified which correspond to the strong- and weak-coupling limits of the exchange with respect to the anisotropy. The strong-coupling case occurs for $j\geq5$, where $u_z$ reaches 1 before the magnetization has had a chance to jump. For this case there is only a continuous rotation of the magnetization permitted. The weak-coupling limit occurs for $j\leq1/2$, where there is only one real solution [$u_z=1$] of Eq. (3) at $h=h_1=2(j-1)$; the magnetization switches from $u_z=1$ directly to $u_z=-1$, which results a ferromagnetic square loop even though there is AF interlayer coupling. In this case the anisotropy controls the switching characteristics

because the exchange coupling is so weak. The hysteresis loops for different values of j are plotted in Fig. 11. Comparison with experiment shows that most of the salient experimental features are reproduced from this calculation.

## IV. Conclusion

In summary, Fe/Mo/Fe and Co/Cu/Cu sandwiches with the Mo and Cu spacer layers fabricated to be wedge shaped have been grown epitaxially with (100) orientation and investigated by the SMOKE technique. The exchange coupling between the two magnetic films oscillates between ferromagnetic and AF as a function of the spacer layer thickness for both systems. For the Fe/Mo system, five oscillations were observed at room temperature in the range of 1-18ML of Mo, with the oscillation periodicity of ~3ML of Mo. For the Co/Cu system, only long-period (5.5ML) oscillations were observed. The AF coupling strength and the oscillation periodicity were shown to be independent of the magnetic layer thickness, indicating that the coupling occurs at the interface of the magnetic and the spacer layers. The hysteresis loops for AF-coupled sandwiches were calculated from a simple model and was shown to reproduce the experimental observations.

Acknowledgment:

The work was supported by U.S. Department of Energy, Basic Energy Sciences-Materials Sciences, under Contract #W-31-109-ENG-38.

Figure Captions:

Fig. 1. The RHEED and LEED patterns for the Mo(100) surface (left), and a Fe(14ML)/Mo(~12ML)/Fe(14ML) wedged sandwich (right).

Fig. 2. RHEED and LEED patterns for the Cu(100) surface (left) and a Co(20ML)/Cu(~10ML)/Co(20ML) wedged sandwich (right).

Fig. 3. Schematic drawing of the fabrication process of a Mo wedge.

Fig. 4. RHEED oscillations during the growth of Co on Cu and Cu on Co.

Fig. 5. Hysteresis loops for different thicknesses of Mo, as denoted to the right. The thickness changes linearly along the length of the wedges.

Fig. 6. The switching field, as defined in Fig. 5, *vs* Mo thickness.

Fig. 7. Hysteresis loops of Co(20ML)/Cu/Co(20ML) for different thicknesses of Cu, as denoted to the right.

Fig. 8. The switching field *vs* Cu thickness.

Fig. 9. The AF-coupling strength $J_{AF} \approx MH_{SD}$ *vs* Cu thickness.

Fig. 10. Schematic drawing of the E-$u_z$ and $u_z$-h curves for different h. The dashed line in the $u_z$-h plane represents $\partial E/\partial u_z = 0$. At $h = h_2 = 8[(j+1)/6]^{3/2}$, where $\partial^2 E/\partial u_z^2 = 0$, the switching occurs from $u_z = [(j+1)/6]^{1/2}$ to $u_z=1$. At $h = h_1 = 2(j-1)$, where $\partial E/\partial u_z = 0$ at $u_z=1$, the switching occurs from $u_z=1$ to $u_z = \{(j/2-1/4)^{1/2}-1/2\}$.

Fig. 11. Calculated hysteresis loops for different j values.

References:


1. P. Grünberg, R. Schreiber, Y. Pang, M. B. Brodsky, and H. Sowers, Phys. Rev. Lett. **57**, 2442 (1986).
2. M. N. Baibich, J. M. Broto, A. Fert, F. Nguyen Van Dau, F. Petroff, P. Etienne, G. Creuzet, A. Friederich, and J. Chazelas, Phys. Rev. Lett. **61**, 2472 (1988).
3. W. R. Bennett, W. Schwarzacher, and W. F. Egelhoff, Jr. Phys. Rev. Lett. **65**, 3169 (1990).
4. M.E. Brubaker, J.E. Mattson, C.H. Sowers, and S.D. Bader, Appl. Phys. Lett. **58**. 2306 (1991).
5. S.S.P. Parkin, N. More, and K.P. Roche, Phys. Rev. Lett. **64**, 2304 (1990).
6. D. Pescia, D. Kerrkmann, F. Schumann, and W. Gudat, Z. Phys. B **78**, 475 (1990); S.S.P. Parkin, R. Bhadra, and K.P. Roche, Phys. Rev. Lett. **66**, 2152, (1991).
7. Y. Wang, P. M. Levy, and J. L. Fry, Phys. Rev. Lett. **65**, 2732 (1990); D. M. Edwards, J Mathon, R. B. Muniz, and M. S. Phan, *ibid.* **67**, 493 (1991); R. Coehoorn, Phys. Rev. B. **44**, 9331 (1991).
8. P. Bruno and C. Chappert, Phys. Rev. Lett. **67**, 1602 (1991); P. Bruno and C. Chappert, Phys. Rev. B. **46**, 261 (1992).
9. J. Unguris, R.J. Celotta, and D.T. Pierce, Phys. Rev. Lett. **67**, 140 (1991).
10. S. T. Purcell, W. Folkerts, M. T. Johnson, N. W. E. McGee, K. Jager, J. ann de Stegge, W. B. Zeper, W. Hoving, and P. Grünberg, Phys. Rev. Lett. **67**, 903 (1991).
11. S. T. Purcell, M. T. Johnson, N. W. E. McGee, R. Coehoorn, and W. Hoving, Phys. Rev. B. **45**, 13064 (1992).

12. A. Fuss, S. Demokritov, P. Grünberg, and W. Zinn, J. Magn. Magn. Mat. **103**, L221 (1992).

13. Z. Q. Qiu, J. Pearson, A. Berger, and S. D. Bader, Phys. Rev. Lett. **68**, 1398 (1992).

14. D.T. Pierce, Bull. Am. Phys. Soc. **37**, 196 (1992).

15. M. Johnson, S. T. Purcell, N. W. E. McGee, R. Coehoorn, J. ann de Stegge, W. Hoving, Phys. Rev. Lett. **68**, 2688 (1992).

16. Z. Q. Qiu, J. Pearson, and S. D. Bader, "Oscillatory Interlayer Magnetic Coupling of Wedged Co/Cu/Co Sandwiches Grown on Cu(100) by Molecular Beam Epitaxy" Phys. Rev. B. **46** (1992) (in press).

17. Z. Q. Qiu, J. Pearson, and S. D. Bader, Phys. Rev. Lett. **67**, 1646 (1991).

18. B. T. Jonker, J. Vac. Sci. Technol. A **8**, 3883 (1990).

19. C. M. Schneider, J. J. Miguel, P. Schuster, R. Miranda, B. Heinrich, and J. Kirschner, in *Science and Technology of Nanostructured Magnetic Materials*, edited by G. C. Hadjipanayis and G. A. Prinz (Plenum, New York, 1991).

20. Z. Q. Qiu, J. Pearson, and S. D. Bader, Phys. Rev. B. **45**, 7211 (1992); Z. Q. Qiu, J. Pearson, and S. D. Bader, *ibid*, **46** (1992) (in press).

21. Z. Q. Qiu, J. E. Mattson, C. H. Sower, H. Welp, S. D. Bader, H. Tang, and J. C. Walker, Phys. Rev. B **45**, 2252 (1992).

22. Y. Yafet, Phys. Rev. B. **36**, 3948 (1987).

23. W. Folkerts, J. of Mag. Mag. Mat. **94**, 302 (1991).

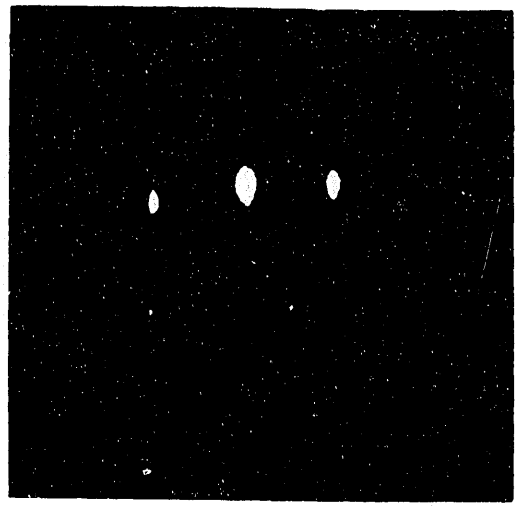

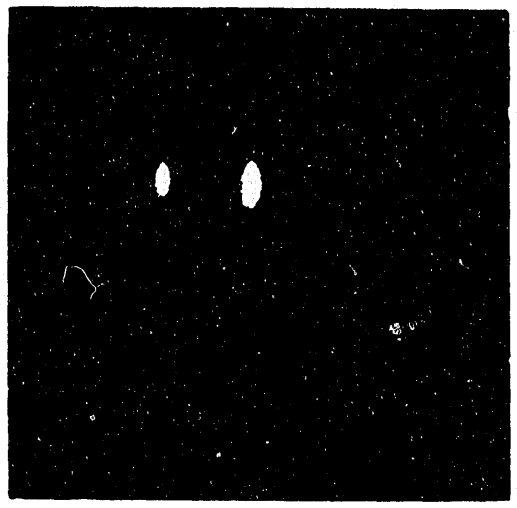

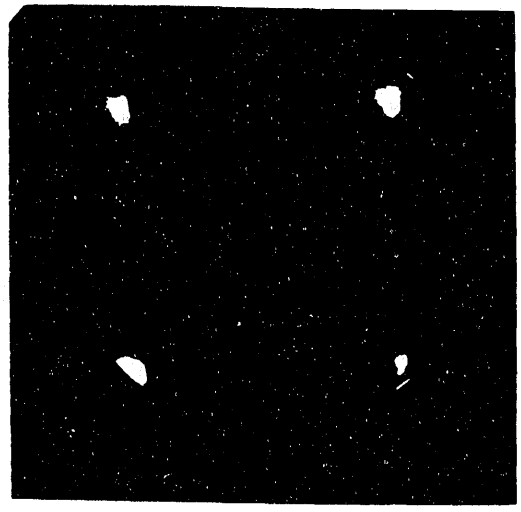

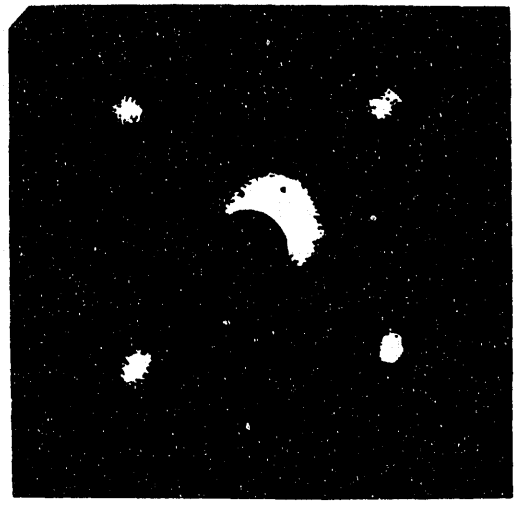

Mo(100)

14Fe/12Mo/14Fe

Fig. 1

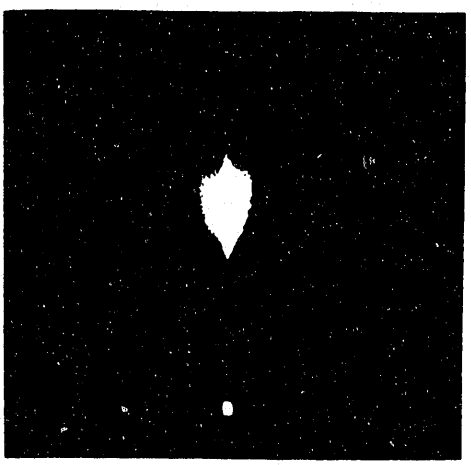

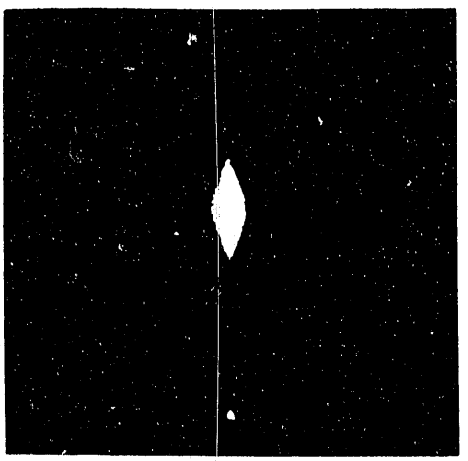

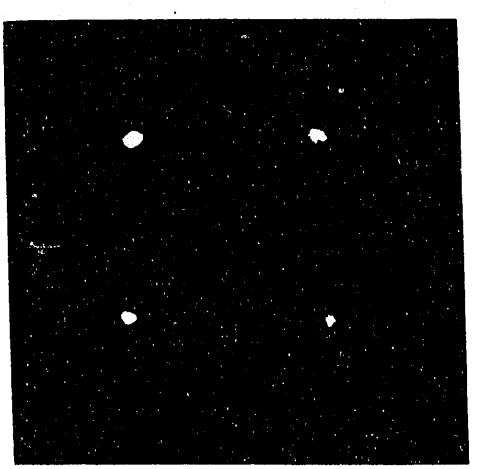

Cu(100)

20Co/nCu/20Co

Fig. 2

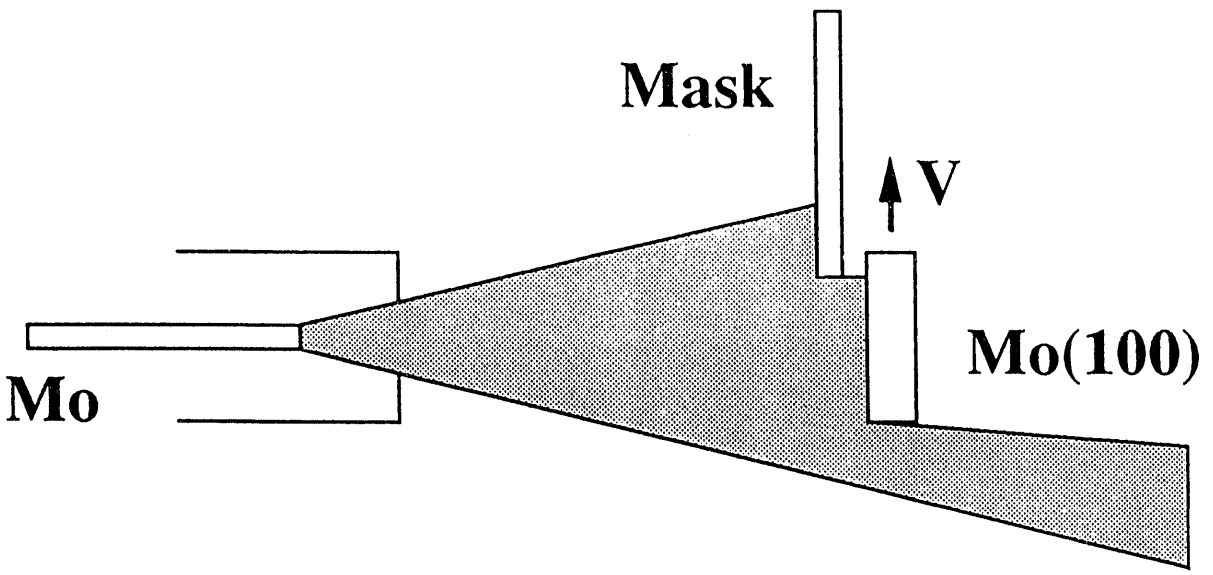


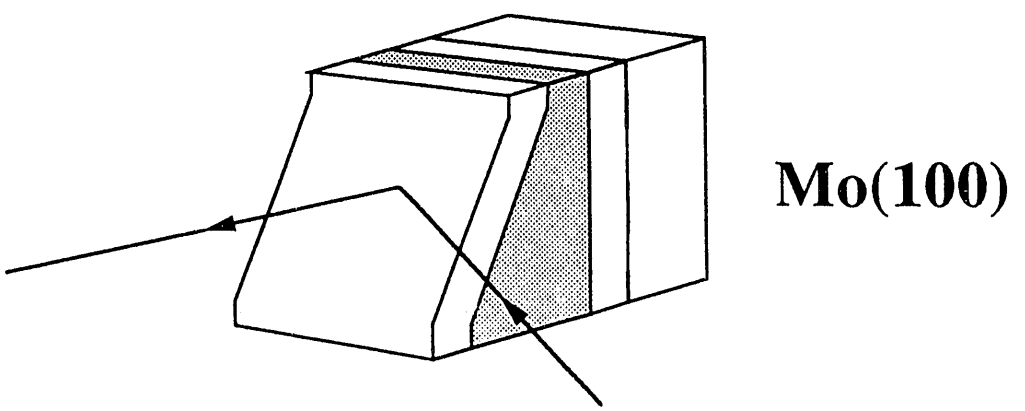


**Mo wedge slope = r/v ~ 1-2Å/mm**

Fig. 3

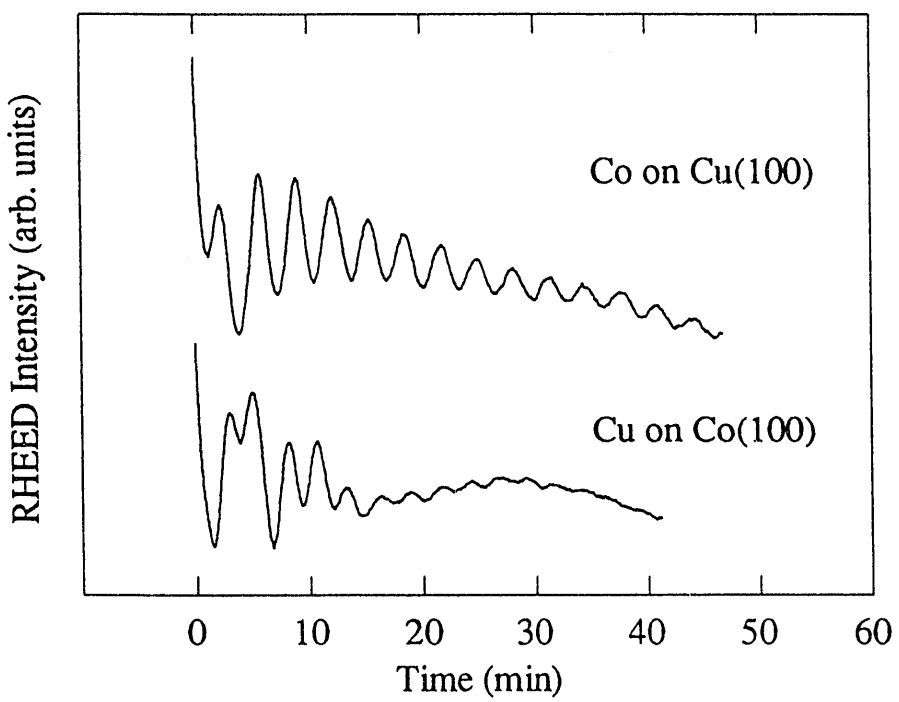
RHEED Intensity (arb. units)
Co on Cu(100)
Cu on Co(100)
0
10
20
30
40
50
60
Time (min)

Fig. 4

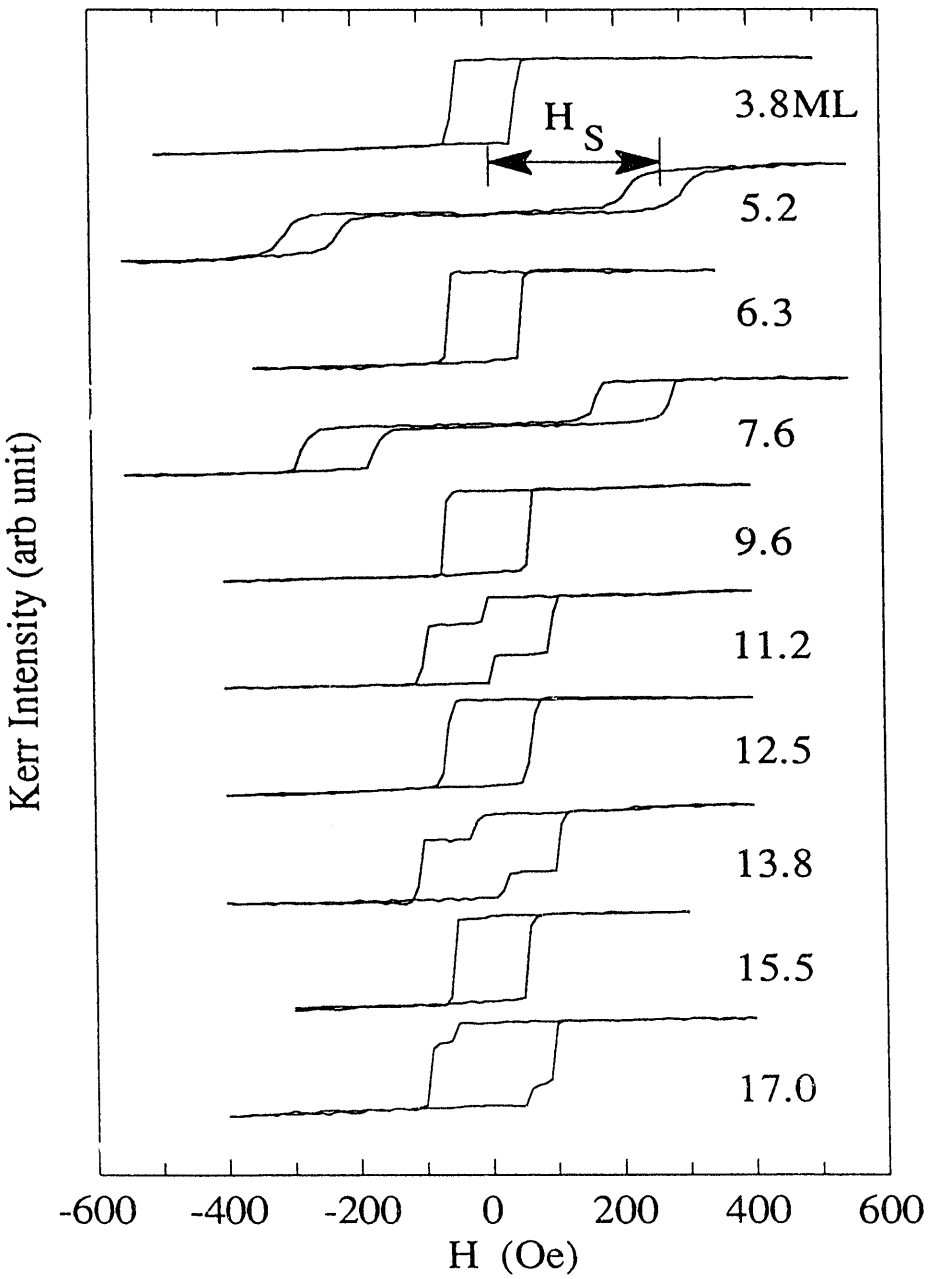
3.8ML
H S
5.2
6.3
7.6
9.6
11.2
12.5
13.8
15.5
17.0
Kerr Intensity (arb unit)
-600
-400
-200
0
200
400
600
H (Oe)

Fig. 5

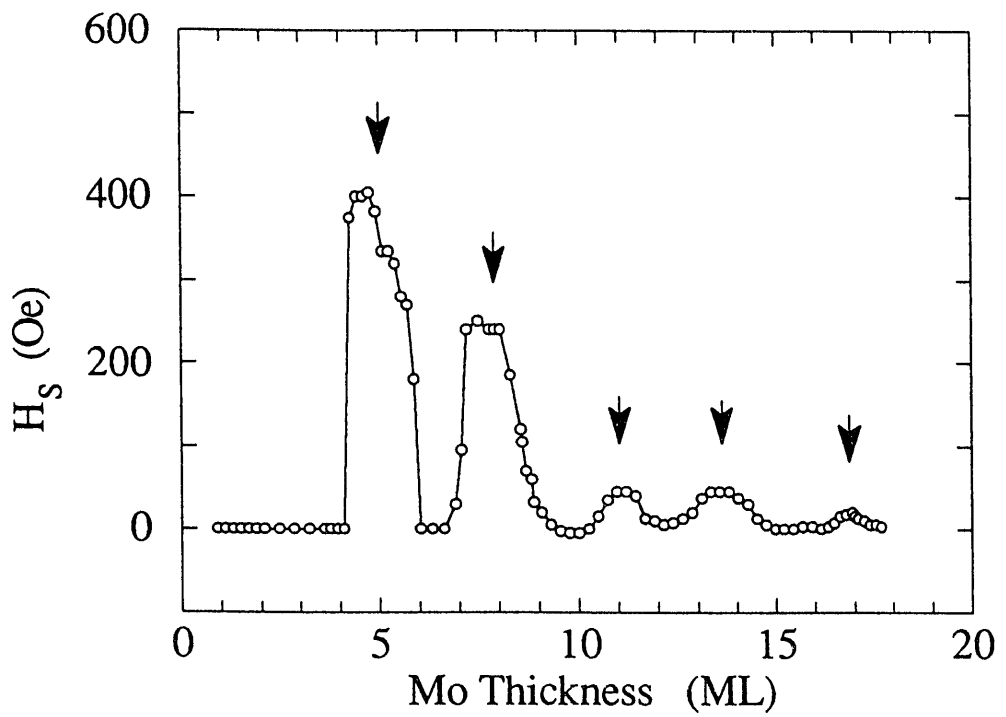


Fig. 6

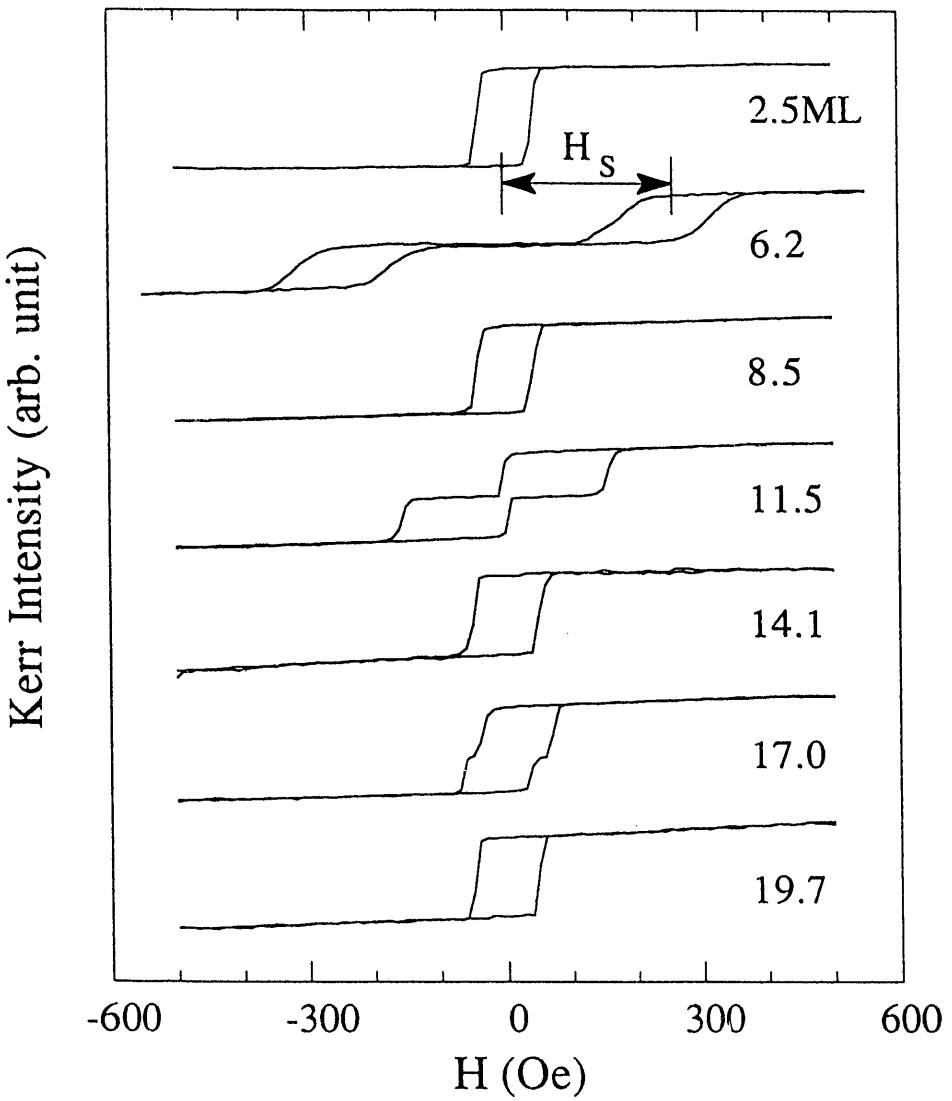
2.5ML
H S
6.2
8.5
11.5
14.1
17.0
19.7
Kerr Intensity (arb. unit)
-600
-300
0
300
600
H (Oe)

Fig. 7

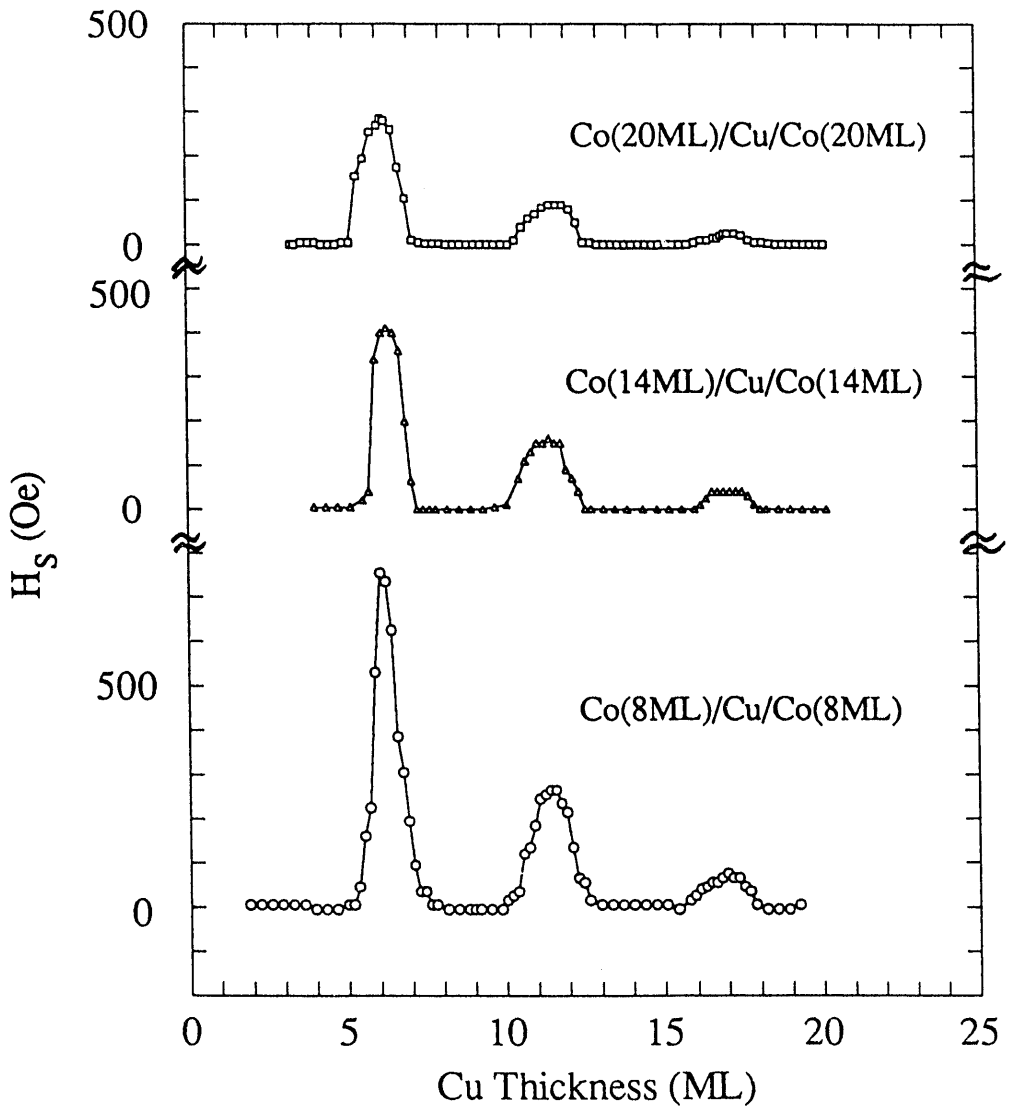
500
0
500
0
500
0
Co(20ML)/Cu/Co(20ML)
Co(14ML)/Cu/Co(14ML)
Co(8ML)/Cu/Co(8ML)
$H_S$ (Oe)
0
5
10
15
20
25
Cu Thickness (ML)

Fig. 8

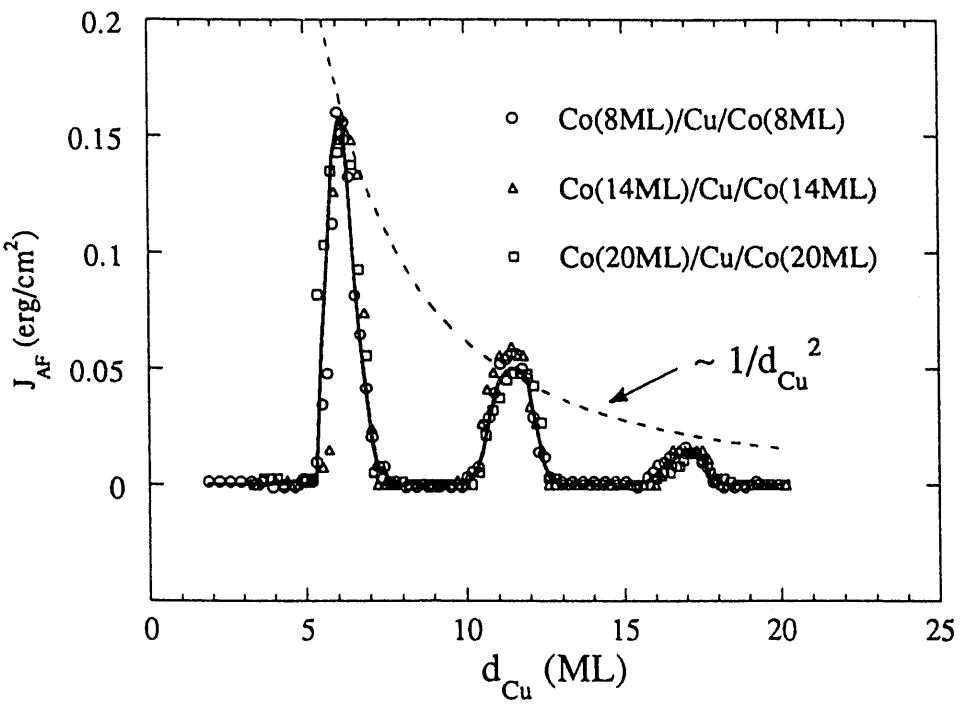
0.2
0.15
0.1
0.05
0
$J_{AF}$ (erg/cm$^2$)
0
5
10
15
20
25
$d_{Cu}$ (ML)
Co(8ML)/Cu/Co(8ML)
Co(14ML)/Cu/Co(14ML)
Co(20ML)/Cu/Co(20ML)
~ $1/d_{Cu}^2$

Fig. 9

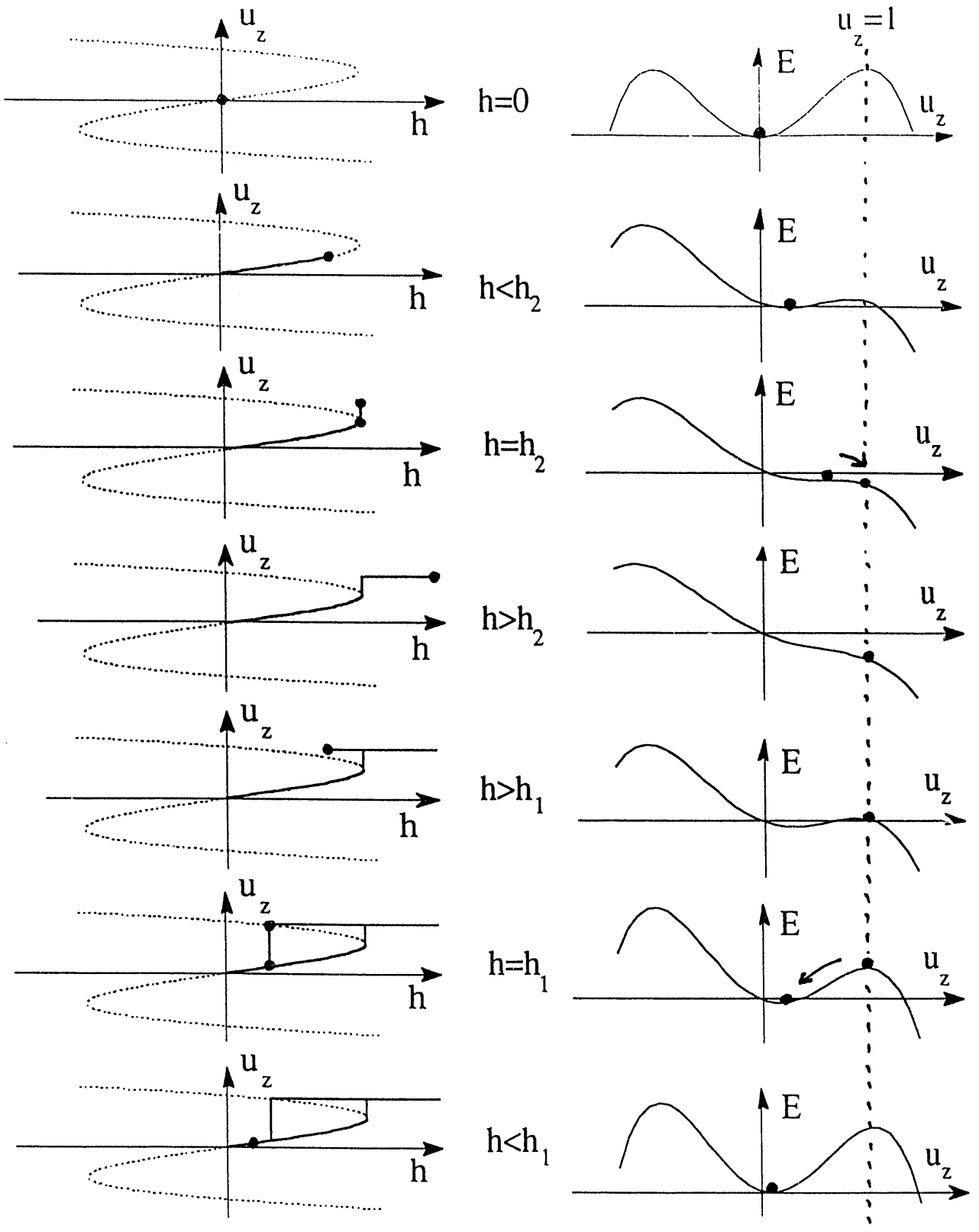


Fig. 10

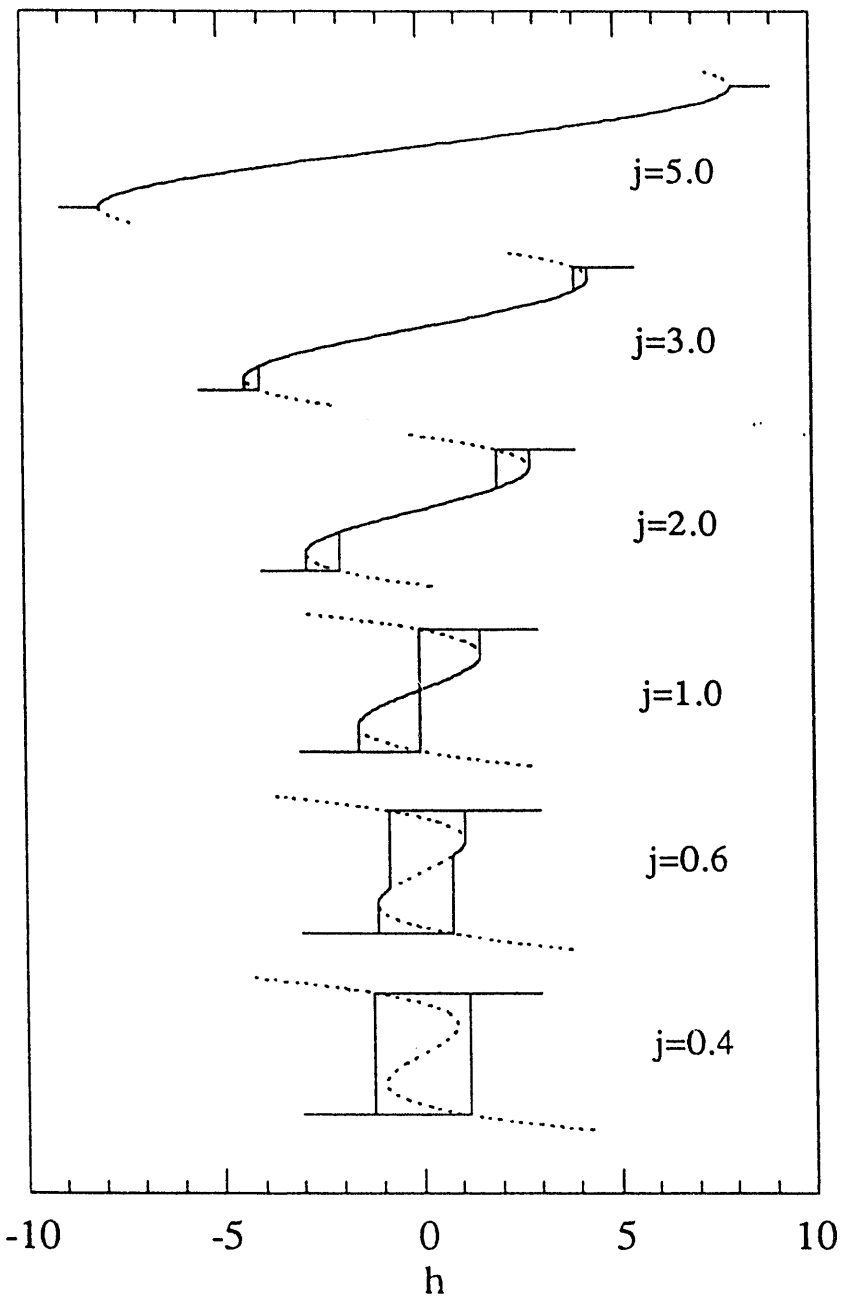


Fig. 11

# END

# DATE FILMED

2/17/93